

**Evolution of vacancy-related defects upon annealing of ion-implanted germanium**

J. Slotte, M. Rummukainen, and F. Tuomisto

*Department of Engineering Physics, Helsinki University of Technology, P.O. Box 1100, FI-02015 HUT, Finland*

V. P. Markevich and A. R. Peaker

*Centre for Electronic Materials, Devices and Nanostructures, University of Manchester, Sackville Street, P.O. Box 88, Manchester M60 1QD, United Kingdom*

C. Jeynes and R. M. Gwilliam

*University of Surrey Ion Beam Centre, Guildford GU2 7XH, United Kingdom*

(Received 2 April 2008; revised manuscript received 23 June 2008; published 1 August 2008)

Positron annihilation spectroscopy was used to study defects created during the ion implantation and annealing of Ge. Ge and Si ions with energies from 600 keV to 2 MeV were implanted at fluences between  $1 \times 10^{12} \text{ cm}^{-2}$  and  $4 \times 10^{14} \text{ cm}^{-2}$ . Ion channeling measurements on as-implanted samples show considerable lattice damage at a fluence of  $1 \times 10^{13} \text{ cm}^{-2}$  and a fluence of  $1 \times 10^{14} \text{ cm}^{-2}$  was enough to amorphize the samples. Positron experiments reveal that the average free volume in as-irradiated samples is of divacancy size. Larger vacancy clusters are formed during regrowth of the damaged layers when the samples are annealed in the temperature range 200–400 °C. Evolution of the vacancy-related defects upon annealing depends noticeably on fluence of ion implantation and for the highest fluences also on ion species.

DOI: [10.1103/PhysRevB.78.085202](https://doi.org/10.1103/PhysRevB.78.085202)

PACS number(s): 61.72.J-, 71.55.Cn, 78.70.Bj

**I. INTRODUCTION**

In recent years we have witnessed a growing interest of germanium as an active element in semiconductor technology. The ever increasing performance demands, with decreasing feature sizes as a consequence, may be better met using germanium. Germanium has higher bulk carrier mobilities than Si or SiGe and in consequence holds the possibility of higher channel mobility in metal-oxide-semiconductor field-effect transistor (MOSFET) devices particularly in the presence of strain.<sup>1</sup> Due to the dominance of silicon in semiconductor industry, very little research has been conducted on the properties of ion-implanted germanium until recently. Some of this work and an extensive comparison of the material properties of silicon and germanium have been compiled by Vanhellefont and Simoen.<sup>2</sup>

Recently Hickey *et al.* reported on defect formation and evolution during regrowth of amorphized ion-implanted Ge.<sup>3</sup> They observed regrowth related defects in annealed 1 MeV Si implanted Ge. End of range defects were minimal and annealed out between 450 and 550 °C while regrowth defects were more stable. In addition their implant conditions were such that a crystalline region remained at the surface resulting in solid phase regrowth occurring from two parallel seed planes resulting in clamshell defects being formed (sometimes called a zipper band) where the two parallel regrowth planes meet. In contrast to Si<sup>4</sup> these defects are more stable than end of range defects.

Positron annihilation spectroscopy (PAS) has been established as a versatile tool for studying open volume defects in semiconductors.<sup>5</sup> However, as with other techniques, very little work has been published on germanium. Positron lifetime studies have been performed on bulk crystals, with defects of monovacancy size reported by Moser *et al.*<sup>6</sup> Vacancy clustering and the annealing of these clusters has been studied by Krause-Rehberg *et al.*<sup>7</sup>

In this work we present results obtained by PAS and supported by Rutherford backscattering spectrometry/channeling (RBS-c) on lattice damage and defects created in ion-implanted highly damaged or amorphized Ge. For all fluences annealing caused the formation of large vacancy clusters. However, after the highest fluence implantations which result in clamshell (or zipper) defect formation, a distinct difference between Si and Ge implanted samples is observed in the annealings.

**II. SAMPLES AND EXPERIMENT**

The samples were Si and Ge implanted Sb-doped *n*-type Ge. The first wafer (samples 1*x*-*x*) was in the  $\langle 100 \rangle$  direction and the resistivity was measured to be  $\rho = 1.6\text{--}1.9 \text{ }\Omega\text{cm}$ . The orientation of the second wafer (samples 2*x*-*x*) was  $\langle 100 \rangle$  tilted 9° toward  $\langle 111 \rangle$  with a resistivity  $\rho = 0.15\text{--}0.17 \text{ }\Omega\text{cm}$ . Six sets of samples were implanted with Si and Ge at fluences  $1 \times 10^{12}\text{--}4 \times 10^{14} \text{ cm}^{-2}$ . The ion energies were 600 keV and 950 keV for Si, and 2 MeV for Ge. The Ge and Si fluences were chosen to yield similar damage, as calculated by TRIM.<sup>8</sup> The implantation depth corresponding to the 950 keV Si ions and 2 MeV Ge ions is approximately 1  $\mu\text{m}$ . The samples were subsequently annealed for 30 min at temperatures 200, 300, 400, and 500 °C in a N<sub>2</sub> atmosphere. For the RBS-c measurements<sup>9</sup> we chose a representative set from the samples used in the PAS study. The samples used in the study are summarized in Table I.

We used a monoenergetic positron beam and the PAS Doppler broadening technique to study defects created by the ion implantation. In Doppler broadening spectroscopy the momentum of the annihilating electron-positron pair is detected as broadening of the 511 keV annihilation peak. We used two Ge detectors with an energy resolution 1.2 keV at

TABLE I. Properties of the studied sample sets. Every set contains an as-implanted sample and samples annealed at 200, 300, 400 and 500 °C for 30 min.

Sample	Template	Ion	Energy	Fluence
11-x	Ge-1	Si	950 keV	$4 \times 10^{13} \text{ cm}^{-2}$
12-x	Ge-1	Ge	2 MeV	$1 \times 10^{13} \text{ cm}^{-2}$
13-x	Ge-1	Si	950 keV	$4 \times 10^{14} \text{ cm}^{-2}$
14-x	Ge-1	Ge	2 MeV	$1 \times 10^{14} \text{ cm}^{-2}$
21-x	Ge-2	Si	600 keV	$1 \times 10^{12} \text{ cm}^{-2}$
22-x	Ge-2	Ge	2 MeV	$1 \times 10^{13} \text{ cm}^{-2}$

511 keV for measuring the annihilation spectra. The annihilation spectra were described using the conventional  $S$  and  $W$  shape parameters.<sup>5</sup> The  $S$  parameter energy window was  $p_\gamma < 3.2 \times 10^{-3} m_0c$ , where  $p_\gamma$  is the momentum of the electron-positron pair. The  $W$  parameter windows were selected as  $12 \times 10^{-3} m_0c < p_\gamma < 30 \times 10^{-3} m_0c$ . The shape parameters reflect the environment of the annihilation site. Typically vacancies are detected as an increase (decrease) of the  $S$  ( $W$ ) parameter from the bulk value. For clusters of a few missing atoms the  $S$  parameter increases almost linearly with the vacancy size in Si.<sup>10</sup> The  $W$  parameter decreases at the same time but the decrease becomes smaller for every missing atom. For large vacancy clusters, however, both parameters saturate. The measured  $S$  and  $W$  parameters are superpositions of  $S$  and  $W$  parameters corresponding to different positron annihilation states in the lattice. Hence, the measured parameters are given by

$$S = \eta_B S_B + \sum \eta_{Di} S_{Di}, \quad (1)$$

$$W = \eta_B W_B + \sum \eta_{Di} W_{Di}, \quad (2)$$

where  $\eta_B$  is the fraction of positrons annihilating in the bulk state and  $\eta_{Di}$  is the fraction of positrons annihilating in the defect state  $i$ .  $S_B$  ( $W_B$ ) and  $S_{Di}$  ( $W_{Di}$ ) are the bulk and defect  $S$  ( $W$ ) parameters, respectively. If a sample contains only two annihilation states, the  $W(S)$  plot of the measurement should form the segment of a line between these states, e.g., bulk and defect state.

For the RBS-c analysis we used a  $^4\text{He}^+$  1.554 MeV ion beam at scattering angles 148.2° and 172.8°. Channeling measurements were done with the beam aligned along the  $\langle 100 \rangle$  channel and with a beam current of approximately 10 nA.

### III. RESULTS AND DISCUSSION

#### A. RBS-c

Figure 1 shows a representative set of the samples studied with RBS-c. As can be observed, the spectrum from the as-implanted sample (Ge fluence  $1 \times 10^{14} \text{ cm}^{-2}$ ) coincides with the random spectrum, indicating that the sample was completely amorphous in the studied depth interval. Reducing the implantation fluence by an order of magnitude resulted in approximately 65%–75% of the atoms being displaced. After annealing at 300 °C a 50 nm-thin crystalline layer is ob-

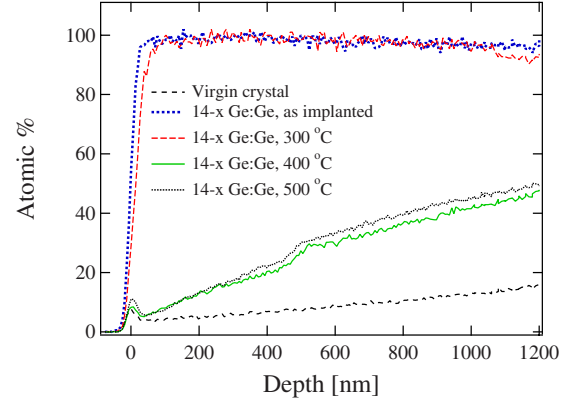


FIG. 1. (Color online) A representative set of the samples studied with RBS-channeling. Also included in the figure is the spectrum from a Ge virgin sample. The clamshell defects can be seen in the samples annealed at 400 °C and 500 °C as a change in slope in the RBS yield at a depth of approximately 500 nm.

served at the surface. An increase in annealing temperature to 400 °C essentially regrows the crystalline structure of the material. However a large number of dislocations is left in the sample. Furthermore the line defects observed are consistent with clamshell defects. The dislocations indicating clamshell defects can be seen as a characteristic change in slope of the RBS yield at a depth of approximately 500 nm. The clamshell defects are also present in the sample annealed at 500 °C, which seems to yield slightly more dechanneled ions than the sample annealed at 400 °C.

The appearance of the clamshell defects at 500 nm, together with a thin crystalline layer observed after the 300 °C anneal, indicate that the ion implantation leaves a crystal seed at the surface. This results in regrowth both from the surface and from the bulk during the annealings.

#### B. PAS

A representative set of the  $S$  parameter as a function of positron implantation energy for as-implanted (fluence  $< 10^{14} \text{ cm}^{-2}$ ) and annealed samples is shown in Fig. 2. The result for all the as-implanted samples, both Ge and Si implanted, was similar. The  $S$  parameter strongly decreased at energies below 5 keV due to positron diffusion and annihilations at the sample surface. As the positron implantation energy was increased, the  $S$  parameter reached a value of  $S/S_B = 1.047$  in the most damaged region. At positron implantation energies above 20 keV, the  $S$  parameter started to decrease as positrons penetrate deeper than the implanted ions, thus probing the defect free Ge bulk. The level of the  $S$  parameter, thus, does not depend on the fluence or on the ion used. This shows that the same types of defects are present and the concentration of positron trapping defects is high enough to produce saturated trapping into open volume defects. Similar saturation of the annihilation parameters after ion implantation has been found earlier in Si.<sup>11</sup>

For annealed Ge implanted (fluence  $1 \times 10^{13} \text{ cm}^{-3}$ ) samples, at energies 5–20 keV, there is a large peak in the  $S$  parameter that corresponds to defects in the implanted layer.

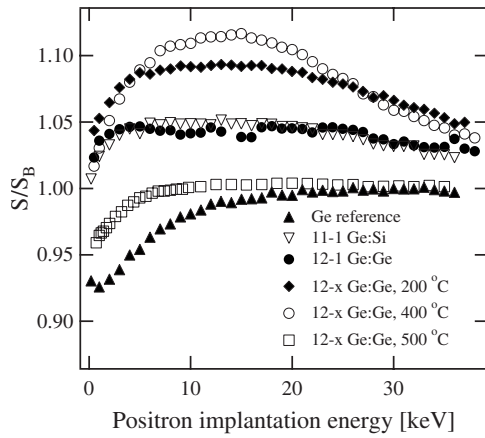


FIG. 2. The low-momentum parameter  $S$  as a function of positron implantation energy for a representative set of as-implanted (fluence  $<10^{14}$  cm $^{-2}$ ) and annealed samples. The data has been scaled to a positron trap free Ge bulk crystal.

The height of this peak increases for annealing temperatures up to 400 °C. After annealing at 500 °C the measured  $S$  parameter is close to that observed in bulk Ge for positron implantation energies above 20 keV; closer to the surface at lower implantation energies the  $S$  parameter is above the parameter for the positron trap free Ge bulk crystal, indicating that there are still open volume defects left after annealing.

Vacancy-donor pairs and divacancies have been found to be mobile in Ge already at the lowest annealing temperature of 200 °C.<sup>12-14</sup> After annealing at 200 °C the  $S$  parameter forms a peak at  $S/S_B \approx 1.09$ , i.e., the difference to the bulk value is doubled from the one recorded in the as-implanted samples. At the same time there is a corresponding decrease in the  $W$  parameter. The  $S$  parameter is closely related to the open volume of the defects. There are very few quantitative PAS studies done in germanium and to make a more exact estimate of the cluster size is therefore difficult. However, a qualitative estimate can be made by using the present results in conjunction with the recent result for the Ge divacancy<sup>15</sup> and by comparing with similar studies in silicon.<sup>10</sup> Hakala *et al.* found an approximately linear relation between the normalized  $S$  parameter and the cluster size. With this approximation and taking into account that the ratio  $\tau_{V_2}/\tau_B$  between the positron lifetime in a divacancy  $\tau_{V_2}$  and in a defect free lattice  $\tau_B$  is similar for Si and Ge, one gets approximately five missing atoms in the samples annealed at 200 °C.

The maximum  $S$  and minimum  $W$  parameter values as a function of annealing temperature from the most damaged region are shown as a function of annealing temperature in Fig. 3. Annealing the samples at 300 °C and at 400 °C increases the  $S$  parameter to  $S \approx 1.11$ . The further increase in the  $S$  parameter suggests that the size of the vacancy clusters increases slightly to six to seven missing atoms. Finally, the  $S$  parameter drops to approximately the level observed in the bulk after an anneal at 500 °C. This shows that most defects anneal out of the sample at 500 °C. This is consistent with earlier studies on annealing of ion implantation damage and recrystallization of amorphous Ge where it has been found that the defects are removed at temperatures

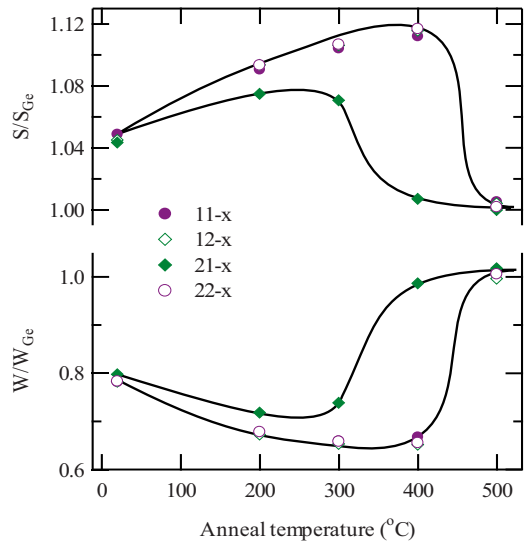


FIG. 3. (Color online) The  $S$  and  $W$  parameter values corresponding to the top of the peak (bottom of the valley) of the  $S$  ( $W$ ) parameter curve as a function of annealing temperature. The data has been scaled to the parameters measured in bulk Ge with  $S_{Ge} = 0.517$  and  $W_{Ge} = 0.036$ .

300–500 °C.<sup>16-18</sup> The annealing temperature of the observed vacancy clusters is similar to what Krause-Rehberg *et al.*<sup>7</sup> found in high-stress and low-temperature deformed high-purity germanium.

It should be noted that the estimates for the cluster sizes are lower limits, since it is assumed that the positron trapping to the clusters is in saturation, i.e., all positrons annihilate in the clusters. The very sharp triangle shaped  $W(S)$ -curve shown in Fig. 4 (12-x, 400 °C) is a clear indication that the positron diffusion length at the depth of the maximum  $S$  parameter is very short, i.e., the positron trapping is in saturation or very close to saturation. Similar sharp triangle shaped curves were obtained for all annealed samples with varying cluster sizes. We therefore estimate that the cluster

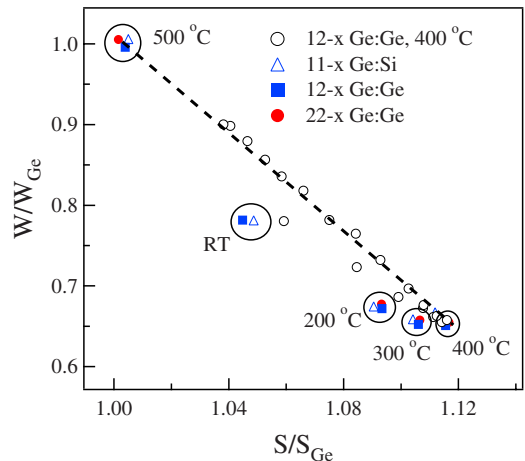


FIG. 4. (Color online)  $W(S)$ -plot for the 12-x sample annealed at 400 °C. Also indicated in the figure are the cluster points for some of the annealed samples. The dashed line indicates the superposition between the bulk and cluster annihilation states.

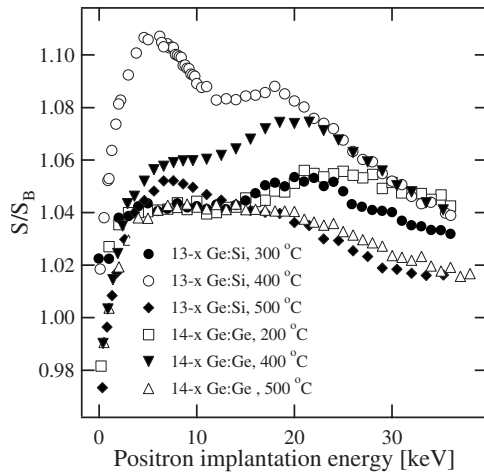


FIG. 5. The low-momentum  $S$  parameter measured at room temperature after 30 min anneal for the set 13- $x$  with Si fluence  $4 \times 10^{14} \text{ cm}^{-2}$  and the set 14- $x$  with Ge fluence  $1 \times 10^{14} \text{ cm}^{-2}$ . The data has been scaled to the parameters measured in bulk Ge with  $S_{\text{Ge}}=0.517$ .

concentration is in the  $10^{17}$ – $10^{18} \text{ cm}^{-3}$  range. Indicated in Fig. 4 is also the turning point from the surface-cluster line to the cluster-bulk line, i.e., the tip of the triangle where the  $S$  parameter is at maximum, for some of the annealings. As can be seen the slope of the cluster-bulk line, indicated for the samples annealed at 400 °C as a dashed line, changes with annealing temperature. This is a clear indication that the defect species changes, i.e., the cluster size changes, with annealing temperature.

Vacancy clustering was observed also in the sample set with the lowest Si fluence  $1 \times 10^{12} \text{ cm}^{-3}$ . Figure 3 shows that in this case the  $S$  parameter increases after the anneal at 200 °C but remains below that observed in the other sample sets. The lower  $S$  parameter can be due to a smaller cluster size or a lower cluster concentration. This is expected when the clusters form through conglomeration of smaller mobile defects and the original defect concentration is lower. After annealing at 300 °C the  $S$  parameter is slightly below the level observed after the 200 °C anneal. In the sample annealed at 400 °C the  $S$  parameter drops to a level  $S=1.007$ , indicating that nearly all the defects were removed in the anneal. The  $S$  parameter decreases further after an anneal at 500 °C and no defects are detected. As can be seen from Fig. 3, no difference in defect evolution is observed between Si and Ge implantation when the estimated implantation damage was equal. In these samples the  $S$  parameter increases with annealing temperatures 200–400 °C while the  $W$  parameter is almost constant. The nonlinear behavior of the  $S$  and the  $W$  parameters shows that the defect type changes in the annealing.

Figure 5 shows the annealing behavior of the samples with the highest implantation fluences for the Si and Ge implantations. The behavior differs significantly from the lower fluences, even though no differences are observed with PAS in the as-implanted samples, i.e., the average open volume does not differ as a result of the ion species or ion fluence. However as can be observed the behavior after annealing is

quite different depending on the ion used in the implantation. RBS-c measurements of the Ge implanted sample showed complete amorphization (Fig. 1); this is also expected for the Si implanted case. Already at 200 °C a peak in the  $S$  parameter starts to develop at a depth of approximately  $1 \mu\text{m}$ . When the annealing temperature is increased to 300 °C a second peak near the surface appears in the silicon implanted sample. This peak continues to grow and reaches approximately the same  $S$  parameter value as the single peak observed in the samples implanted with a lower fluence. The peak at  $1 \mu\text{m}$  grows with increasing annealing temperature for both the silicon and germanium implantation and shows a slight shift toward the surface. The height of the deeper peak is approximately  $1.08 \times S_B$ , i.e., lower than in the samples implanted with lower fluences. The behavior of the open volume defects at depths around  $1 \mu\text{m}$  for both the Ge and Si implanted case can be explained by the appearance of the clamshell defects at 500 nm, which prevent the formation of larger vacancy clusters beyond the clamshell defects, i.e., vacancy-vacancy defect interaction is suppressed. A probable explanation for the distinct difference in behavior above the clamshell defects, with apparently smaller open volume defects in the Ge implanted case and with large vacancy clusters forming during annealings at 200–400 °C, is the difference in deposited energy in this region during ion implantation. For the heavier and more energetic Ge ion the deposited energy in the track region of the ions will be much larger than for the lighter and less energetic Si ion, even though the calculated damage in the end of range is similar for the two cases. Even though both implantations result in an amorphous layer, differences can occur in the seed for regrowth at the surface, or there could be more ordered structures left in the Si implanted case. Also noteworthy is that the open volume defects are found in both samples and in both regions, above and beyond the clamshell defects, even after annealing at 500 °C.

#### IV. CONCLUSIONS

In summary, we have studied implantation damage in Si and Ge implanted Ge, with the ion fluence varying between  $1 \times 10^{12} \text{ cm}^{-2}$  and  $4 \times 10^{14} \text{ cm}^{-2}$ . Positron annihilation spectroscopy and Rutherford backscattering/channeling have been used for characterization of lattice damage, extended and point defects. In the as-implanted samples, channeling measurements show considerable lattice damage at a fluence of  $1 \times 10^{13} \text{ cm}^{-2}$  and a fluence of  $1 \times 10^{14} \text{ cm}^{-2}$  was enough to amorphize the crystal structure. Positron annihilation spectroscopy in the Doppler broadening mode gives the annihilation parameters  $S=1.047$  and  $W=0.79$  independently of ion and fluence for the as-implanted samples. The annihilation parameters indicate an average free volume approximately of divacancy size. In annealed layers channeling measurements show recovery of the damaged region beginning from the surface and vacancy clustering is detected by positrons. The cluster size depends on the fluence. Annealing at 500 °C was enough to remove all the defects when the ion fluence was below  $4 \times 10^{13} \text{ cm}^{-2}$ . For samples implanted with fluences above  $10^{14} \text{ cm}^{-2}$ , channeling measurements revealed clamshell defects at a depth of approximately 500

nm. These clamshell (or zipper) defects strongly influence the annealing behavior of open volume defects. Also a difference between Si and Ge implants in the near surface region is observed. This difference is explained by differences in the deposited energy during implantation in this region of the samples.

## ACKNOWLEDGMENTS

We would like to thank Umicore for providing the germanium wafers. The authors wish to acknowledge the contribution of the late Professor Kimmo Saarinen.

- 
- <sup>1</sup>M. L. Lee, E. A. Fitzgerald, M. T. Bulsara, M. T. Currie, and A. Lochtefeld, *J. Appl. Phys.* **97**, 011101 (2005).
- <sup>2</sup>J. Vanhellemont and E. Simoen, *J. Electrochem. Soc.* **154**, H572 (2007).
- <sup>3</sup>D. P. Hickey, Z. L. Bryan, K. S. Jones, R. G. Elliman, and E. E. Haller, *Appl. Phys. Lett.* **90**, 132114 (2007).
- <sup>4</sup>K. S. Jones, S. Prussin, and E. R. Weber, *Appl. Phys. A: Solids Surf.* **45**, 1 (1988).
- <sup>5</sup>K. Saarinen, P. Hautojärvi, and C. Corbel, in *Identification of Defects in Semiconductors*, edited by M. Stavola (Academic, New York, 1998), p. 209.
- <sup>6</sup>P. Moser, J. L. Pautrat, C. Corbel, and P. Hautojärvi, in *Positron Annihilation*, edited by P. C. Jain, M. Singru, and K. P. Gopinathan (World Scientific, Singapore, 1985), p. 733.
- <sup>7</sup>R. Krause-Rehberg, M. Brohl, H. S. Leipner, Th. Drost, A. Polity, U. Beyer, and H. Alexander, *Phys. Rev. B* **47**, 13266 (1993).
- <sup>8</sup>J. F. Ziegler, J. P. Biersack, and U. Littmark, *The Stopping and Range of Ions in Solids* (Pergamon, New York, 1985).
- <sup>9</sup>A. Simon, C. Jeynes, R. P. Webb, R. Finnis, Z. Tabatabaian, P. J. Sellin, M. B. H. Breese, D. F. Fellows, R. van de Broek, and R. M. Gwilliam, *Nucl. Instrum. Methods Phys. Res. B* **219-220**, 405 (2004).
- <sup>10</sup>M. Hakala, M. J. Puska, and R. M. Nieminen, *Phys. Rev. B* **57**, 7621 (1998).
- <sup>11</sup>B. Nielsen, O. W. Holland, T. C. Leung, and K. G. Lynn, *J. Appl. Phys.* **74**, 1636 (1993).
- <sup>12</sup>V. P. Markevich, I. D. Hawkins, A. R. Peaker, K. V. Emtsev, V. V. Emtsev, V. V. Litvinov, L. I. Murin, and L. Dobaczewski, *Phys. Rev. B* **70**, 235213 (2004).
- <sup>13</sup>P. Ehrhart and H. Zillgen, *J. Appl. Phys.* **85**, 3503 (1999).
- <sup>14</sup>A. R. Peaker, V. P. Markevich, L. I. Murin, N. V. Abrosimov, and V. V. Litvinov, *Mater. Sci. Eng., B* **124-125**, 166 (2005).
- <sup>15</sup>K. Kuitunen, F. Tuomisto, J. Slotte, and I. Capan, *Phys. Rev. B* **78**, 033202 (2008).
- <sup>16</sup>L. Csepregi, R. P. Küllen, J. W. Mayer, and T. W. Sigmon, *Solid State Commun.* **21**, 1019 (1977).
- <sup>17</sup>A. Satta, E. Simoen, T. Clarysse, T. Janssens, A. Benedetti, and B. de Jaeger, *Appl. Phys. Lett.* **87**, 172109 (2005).
- <sup>18</sup>I. Suni, G. Göltz, M.-A. Nicolet, and S. S. Lau, *Thin Solid Films* **93**, 171 (1982).